Journal of Alloys and Compounds 690 (2017) 169–175

Contents lists available at ScienceDirect

Journal of Alloys and Compounds

journal homepage: http://www.elsevier.com/locate/jalcom

Pseudogap of Ortho-III $YBa_2Cu_3O_{7-x}$ from Cu EPR investigation

Min-Quan Kuang [a], Shao-Yi Wu [b], Hong-Kuan Yuan [a], Li-Dan Wang [c], Shu-Kai Duan [c, *], An-Long Kuang [a], Guo-Qing Li [a]

[a] School of Physical Science and Technology, Southwest University, Chongqing 400715, China
[b] Department of Applied Physics, School of Physical Electronics, University of Electronic Science and Technology of China, Chengdu 610054, China
[c] College of Electronic and Information Engineering, Southwest University, Chongqing 400715, China

ARTICLE INFO

Article history:
Received 25 March 2016
Accepted 5 August 2016
Available online 7 August 2016

Keywords:
Pseudogap
Pseudo Jahn-Teller effect
Electron paramagnetic resonance (EPR)
$YBa_2Cu_3O_{7-x}$

ABSTRACT

The temperature dependences of g factors of underdoped $YBa_2Cu_3O_{7-x}$ ($T_c \approx 86.5$ K) indicate that the pseudogap onset temperature T^* (≈ 190 K) coincides with the phase boundary established by resistivity, Nernst effect, neutron diffraction and ultrasound measurements in YBCO phase diagram. The obtained empirical relationship between g factors and pseudogap is appropriate for the entire charactering temperature range of Ortho-III YBCO. The EPR signals are ascribed to the localized $Cu^{2+}(1)$ sites based on the quantitative calculations of the g factors by involving the local structures of the paramagnetic copper (1) sites. The present work provides another potential spectroscopic probe for the pseudogap in underdoped high T_c superconductors and the origin of EPR and related mechanisms in YBCO which are still controversial.

1. Introduction

The cuprate superconductors which possesses novel properties in superconductivity [1,2], mechanics [3], magnetics [4] and electronic structure [5] is the most favorable candidate for applications in heterojunctions [6], Josephson-junctions [7–9], detectors [10] and coated conductors [11]. Among these unique properties, the nature of pseudogap (PG) in cuprate superconductors is a crucial issue to understand the suppression of transition temperature (T_c) [12–14] in the noted 60 K and 90 K plateaus where n_p, the hole concentration per planar CuO_2, ranges from 0.09 to 0.15 [15]. Recent works reveal that PG arises from the competition between superconductivity and order phases, such as stripe or nematic order [14], spin or charge density wave (SDW/CDW) [16,17], and symmetry breaking (time-reversal, rotational and C_4 symmetry) [12,13]. The corresponding temperature T^* where PG occurs has been demonstrated by various experiments such as resistivity [12], Nernst effect and neutron diffraction [16] and ultrasound [18]. The phase diagrams of $YBa_2Cu_3O_y$ ($0.35 \leq y \leq 1$) exhibit PG monotonically decreases to zero with increasing n_p from 0.08 to 0.19 in the superconducting dome [14,16,18]. Normally, the absence of PG reported in EPR study is attributed to the conventional conjecture that copper in pure single phase high T_c superconductors is EPR silent due to the suppression of paramagnetivity by antiferromagnetism (superconductivity) [19–21]. Whereas the origins of the observed axial EPR g factors are likely ascribed to impurities or parasitic phase (e.g., Y_2BaCuO_5 and $BaCuO_{2+x}$) and the six-coordinated pseudooctahedra on Cu(1) sites or paramagnetic chain fragments (PCF) in CuO chains [19,20,22–25]. Therefore, the above problem of assignment of EPR signals in cuprate superconductors is worthy to be further clarified. Of course, signals of paramagnetic centers can be completely suppressed or shielded under superconducting state. Nevertheless, since the temperature of zero resistance may vary with different samples, the signals of paramagnetic centers may not be completely depressed and thus can be detected for the orthorhombic phases by EPR measurements [26]. Along this line, EPR signals would be detectable in the zones (i.e., CDW zone) where superconductivity is depressed, and observability of EPR can depend upon the degree of depression of the paramagnetic centers by superconductivity (or the degree of depression of superconductivity by other mechanisms). In present work, the temperature dependent anisotropic g factors are theoretically studied for ortho-III $YBa_2Cu_3O_{7-x}$ in view of PG deeply entwined with CuO_2 planes by connecting the local structures of $Cu^{2+}(1)$ sites. And the possibility of EPR signal in ortho-III $YBa_2Cu_3O_{7-x}$ ($T_c \approx 86.5$ K [26]) stemming from defects or impurities is excluded.

* Corresponding author.
E-mail address: duansk@swu.edu.cn (S.-K. Duan).

http://dx.doi.org/10.1016/j.jallcom.2016.08.044
0925-8388/

2. Analysis and calculations

2.1. EPR phenomenon in YBCO

As for the effective characterization methods for cuprate superconductors, EPR can be the alternative measurement probed by Cu^{2+} or other paramagnetic cations. The EPR signals for deficient oxygen samples of $YBa_2Cu_3O_{7-x}$ polycrystalline pellets were measured at 77–300 K and the temperature dependent anisotropic gyromagnetic factors g_i (i = x, y and z labeling the directions along a, b and c axes, respectively) were obtained [26]. As one can see from Fig. 1, g_i experience continuous decreases with increasing temperature until 189 K and then exhibit a smooth variation. The distinct fluctuations occur around T_c (≈86.5 K) and the orthorhombic structure is evidenced by the principal g values g_x, g_y and g_z at 77 K. The EPR signals most likely originate from the named green phase Y_2BaCuO_5 and/or $BaCuO_{2+x}$ coming from the preparation processes. Reports [19,27] reveal that the Neel temperature (T_N) for Y_2BaCuO_5 and $BaCuO_{2+x}$ are about 40 K and 15 K, respectively, and both can be detected in the EPR measurements when embedded in the samples. Since the EPR spectra should be of tetragonal and orthorhombic symmetries for Y_2BaCuO_5 and $BaCuO_{2+x}$, respectively [19,28], the observed axial g signals can be attributed to the axial Cu^{2+} sites of tetragonal phase rather than insulator phase [26].

Since no satisfactory theory has been introduced to elaborate the intriguing phenomenon of EPR silence for Cu^{2+} in various HTSCs [19], we confine present work to the YBCO systems with hole doping. Based on the typical EPR silence, axial g factors of $YBa_2Cu_3O_y$ systems (see Table 1) [19,22–26,29–32] and the structure phase of YBCO (list in Table 2) [33,35–37], one can classify these samples into the tetragonal ($y < 0.35$) and orthorhombic phases ($0.35 \leq y \leq 1$). The EPR signals are observable under appropriate doping ($0.05 \leq y \leq 0.23$) for the tetragonal phase [25,29] where T_N is nearly constant for $y \leq 0.2$ [34]. The orthorhombic phase is approximately separated into 5 second order phases named Ortho-I, Ortho-II, Ortho-III, Ortho-V and Ortho-VIII phases, according to the respective oxygen-ordering superstructures with different phase transition temperatures T_P [33,35–37]. Partial observable EPR spectra of given samples for doping less than 0.08 per planar CuO_2 in the tetragonal [25,29] and Ortho-II [23,24] phases can be attributed to the paramagnetic centers related to the spin order which suppress the superconductivity and bridge the antiferromagnetic (AF) and the superconducting phase [38–40]. Varying dramatically from 60 K to 90 K plateau, the hole concentration n_p per planar CuO_2 can be estimated from the empirical formula related to the c-axis lattice parameter [15]. The named 60 K samples [22,25,30] locate in the Ortho-V and/or Ortho-VIII phases where the superstructures may be simply treated as the reconfiguration of Ortho-II and Ortho-III phases [33]. Despite most EPR spectra for 90 K specimens [23,29–31] are absent, Ref. [32] reports analogous EPR behaviors to the sample of Ortho-III phase [26]. The disappearance of orthorhombic signal [32] would be illustrated as the competition between different oxygen-orderings and the suppression coming from Ortho-I phase in the superconducting dome. It is noticeable that EPR emergence situates in Ortho-V, Ortho-VIII and Ortho-III regions with $0.09 \leq n_p \leq 0.15$ [15] and the competition between charge order and superconductivity gives rise to appearance of electronic pockets which bring forward reconstruction of Fermi surface [16,17,38,40]. The issue whether EPR spectra are related to the charge order and/or the Ortho-III superstructure is extremely complicated and fairly extensive and thus beyond the scope of present work. However, it is straightforward to achieve the conjecture that there is no doubt about the existence of the EPR spectra for $YBa_2Cu_3O_y$ system and the most probable nominees related to the paramagnetic center are the spin order for the low doping region ($n_p < 0.08$), and the charge order and/or the Ortho-III superstructure (Full-Full-Empty alternating CuO chains) for the underdoped region. No EPR reports referring to the thermodynamically stable Ortho-VIII and Ortho-III superstructure (optimal doping at $n_p \approx 0.123$ and 0.133, respectively [15,33,37]) have been presented, and one reasonable substitute is the EPR spectra for $YBa_2Cu_3O_{7-\delta}$ (Tc ≈ 86.5 K) [26] which happens to lie in the Ortho-III phase.

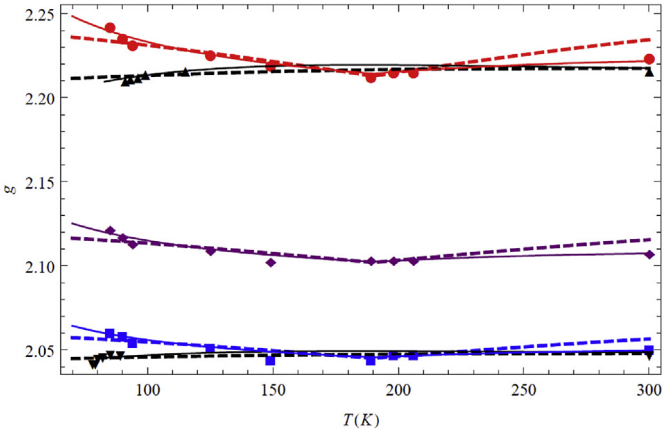

Fig. 1. Temperature dependent g factors of Y123. The circles, squares and diamonds denote, respectively, $g_{//}$, $g_\perp$ and g_{eff} for $YBa_2Cu_3O_{7-x}$ ($T_c \approx 86.5$ K) [26]. The up and down triangles are the anisotropic g factors for $YBa_2Cu_3O_{7-\delta}$ ($T_c \approx 91$ K) [32]. The dashed lines are fitted by PG (≈190 and 91 K for $YBa_2Cu_3O_{7-x}$ and $YBa_2Cu_3O_{7-\delta}$, respectively) with the linear function α_i |Tanh $(1 - T/T^*)$| + g_i (T^*). The solid line represents the modification with $\alpha_i T^{-1}$ |Tanh $(1 - T/T^*)$| + g_i (T^*).

2.2. Determination of PG and fitting of g factors in a phenomenological way

The observed EPR signal in the normal state can be ascribed to Cu^{2+} ($3d^9$), with the opposite variation tendency of the anisotropic g factors to the nuclear spin relaxation rate $1/T_1T$ and Knight shift [39,41,42] where the opening of the PG at T^* is corresponding to the peak of the observed curves. More reasonable definition of PG is given as the onset of negative deviation for linear temperature dependence in-plane resistivity at high temperature [12]. Then, the derivative $D_i(T) \equiv (g_{i,j} - g_{i,k})/(T_j - T_k)$ is plotted in Fig. 2, where $T_j > T_k$ for the anisotropic g_i (i = //and ⊥). One can find that $D_i(T)$ normalizes to zero at high temperature and $T^\dagger \approx 190$ K where D(T) changes sign for $YBa_2Cu_3O_{7-x}$ ($T_c \approx 86.5$ K) coincides with T^* acquired from other measurements [12,16,18] within errors in the YBCO phase diagram (see Fig. 3). In Fig. 2, the filled up and down triangles are taken from optimal doping $YBa_2Cu_3O_{7-\delta}$ ($T_c \approx 91$ K) [32] where PG approaching to the superconducting gap (SG) [41]. The discrepancy between the in-plane $D_{//}(T)$ and the out-of plane $D_\perp(T)$ for $YBa_2Cu_3O_{7-\delta}$ ($T_c \approx 91$ K) can be attributed to the variant completion between superconductivity and antiferromagnetic correlation compared to $YBa_2Cu_3O_{7-x}$ ($T_c \approx 86.5$ K) which presents uniform D(T) well above T_c. For $YBa_2Cu_3O_{7-x}$ ($T_c \approx 86.5$ K), Fig. 2 shows the fluctuation of D(T) before changing sign, with $T^\dagger$ varying from nearly 192 K to 189 K for out-of plane and in-plane, respectively. As regards $YBa_2Cu_3O_{7-\delta}$ ($T_c \approx 91$ K), however, $T^\dagger$ experiences the large anisotropy of almost 91 or 78 K along *c* or *a* (*b*) axes, respectively.

Since the gained $T^\dagger$ happens to lie in the boundary of the PG, one can tentatively elucidate the g factors in terms of PG. Based on the simulations for $1/T_1T$ and NMR curves [41,42] and the linear